

Benchmarking Federated Learning for Semantic Datasets: Federated Scene Graph Generation

SeungBum Ha^{1,*}, Taehwan Lee^{1,*}, Jiyouon Lim³, Sung Whan Yoon^{1,2,†}

¹Graduate School of Artificial Intelligence, Ulsan National Institute of Science and Technology, Ulsan, Korea

²Department of Electrical Engineering, Ulsan National Institute of Science and Technology, Ulsan, Korea

³Electronics and Telecommunications Research Institute (ETRI), Daejeon, Korea

{ethereal0507, taehwan, shyoon8}@unist.ac.kr, {kusses}@etri.re.kr

Abstract—Federated learning (FL) has recently garnered attention as a data-decentralized training framework that enables the learning of deep models from locally distributed samples while keeping data privacy. Built upon the framework, immense efforts have been made to establish FL benchmarks, which provide rigorous evaluation settings that control data heterogeneity across clients. Prior efforts have mainly focused on handling relatively simple classification tasks, where each sample is annotated with a one-hot label, such as MNIST, CIFAR, LEAF benchmark, etc. However, little attention has been paid to demonstrating an FL benchmark that handles complicated semantics, where each sample encompasses diverse semantic information from multiple labels, such as Panoptic Scene Graph Generation (PSG) with objects, subjects, and relations between them. Because the existing benchmark is designed to distribute data in a narrow view of a single semantic, e.g., a one-hot label, managing the complicated *semantic heterogeneity* across clients when formalizing FL benchmarks is non-trivial. In this paper, we propose a benchmark process to establish an FL benchmark with controllable semantic heterogeneity across clients: two key steps are i) data clustering with semantics and ii) data distributing via controllable semantic heterogeneity across clients. As a proof of concept, we first construct a federated PSG benchmark, demonstrating the efficacy of the existing PSG methods in an FL setting with controllable semantic heterogeneity of scene graphs. We also present the effectiveness of our benchmark by applying robust federated learning algorithms to data heterogeneity to show increased performance. Our code is available at <https://github.com/Seung-B/FL-PSG>.

Index Terms—Scene Graph Generation, Panoptic Scene Graph Generation, Federated Learning, Distributed Learning, Data Privacy, Benchmark

I. INTRODUCTION

Federated learning (FL) has drawn great attention as a key framework for enabling decentralized training of deep models from the distributed private data to numerous edge clients. The FL framework communicates the model parameters between the clients and the server; to keep the distributed local data private, the server cannot access data samples of clients [1]. This property of FL that preserves data privacy makes it more crucial when deep models for tasks with license- or privacy-sensitive data, such as clinical data from medical institutions, private information from electronic edge devices, licensed contents from providers, and broadcasting stations, etc.

*Equal Contribution

†Corresponding Author

This work has been submitted to the IEEE for possible publication.

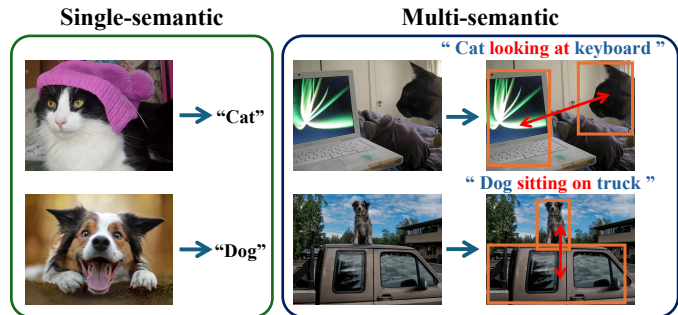


Fig. 1. Examples of **Single-semantic** (Left: image classification) and **Multi-semantic** (Right: scene graph generation) tasks.

Along with the rapid advancement of the algorithmic development of FL, great efforts have been dedicated to constructing FL benchmarks that allow reliable and rigorous evaluations for the existing FL methods. The existing FL benchmarks mostly rely on the existing datasets, including MNIST [2], CIFAR [3], CelebA [4], Twitter [5], etc, then building upon them, researchers focus on devising a decentralized training setting with controllable factors, such as data heterogeneity across clients, number of clients, ratio of participating clients, number of the maximum communication rounds, etc.

Among the factors of FL settings, *data heterogeneity* works as the most crucial factor that obviously exhibits the efficacy of different FL algorithms; when the data distribution strongly deviates across clients, a federation of local models typically fails with drastic performance drops [6]. To construct a controllable and rigorous benchmark process with data heterogeneity, researchers intentionally diversify the prior distribution of one-hot label of samples across clients via random sampling of the priors from Dirichlet distribution [7], [8], or shard- or chunk-wise assignment of data [1].

Herein, we want to point out two key limitations of the existing FL benchmarks. Firstly, the current benchmarks mostly handle simple classification or regression tasks, where each sample is paired with a one-hot label or a single target value. However, deep training tasks currently become far beyond mere classification or recognition and consider highly complicated jobs to understand in-depth semantic information hidden in the given data sample, e.g., generating realistic samples

[9], [10], finding similar samples [11]–[13] from the prompts, or answering the queries about actions and objects shown in photos [14], [15]. Extending the current FL benchmark process to tasks that consider complicated semantics is necessary.

Second, there does not exist a task-agnostic FL benchmark process that devises controllable *semantic heterogeneity* of data across clients. In a simple image classification FL benchmark, for instance, the existing process focuses on a single semantic, i.e., the class label, and deviates the label distribution across clients to devise data heterogeneity (referring to the left image of Fig. 1). In contrast, devising data heterogeneity is non-trivial when considering vision tasks, where each sample contains multiple semantics. As shown in the right image of Fig. 1, Scene Graph Generation, which is a core vision task for understanding the complicated semantics of a given image, a single sample bears multiple objects ('cat', 'keyboard', 'dog' and 'truck'), predicates ('looking at' and 'sitting on') and relations ('cat' \rightarrow 'keyboard', 'dog' \rightarrow 'truck'). Partitioning samples with such complex semantics into clients while controlling the semantic heterogeneity remains unexplored.

In this study, we propose an FL benchmark process that enables the evaluation of FL algorithms on multi-semantic datasets while controlling semantic heterogeneity. To break the aforementioned limitations, our process encompasses two key steps: i) discovering the semantic clusters by utilizing the collection of multiple annotations called 'category tensor'. ii) distributing data samples to multiple clients by considering the heterogeneity between the different semantic clusters.

As a proof of concept, we aim to construct the FL benchmark for the Panoptic Scene Graph Generation (PSG) task, a family of scene graph generation tasks that utilize the panoptic segmentation, i.e., segmented objects, not the bounding boxes. And classic scene graph generation tasks use a bounding box-based object grounding. However, the bounding box contains more noise than the pixel-level object. In scene graph generation, inferring relationships between objects is crucial. Panoptic segmentation provides precise boundary information, allowing better computation of distances or overlaps between objects. We select the PSG task because discovering scene graphs not only directly links to the fundamental understanding of visual perceptions but also works as a key module in bridging vision and language [16].

To the best of our knowledge, our work first attempts to establish the FL benchmarks for the PSG and provides the evaluation results that demonstrate the effectiveness of the existing PSG baselines in decentralized training settings. The simulation results reveal that the methods tailored to tackle the long-tailed problem in the PSG task, where some objects and predicates are more dominant than others, are robust in handling semantic heterogeneity in FL.

II. RELATED WORKS

A. Federated Learning (FL) and Benchmarks

FL has emerged as a pivotal framework for training deep learning models in a decentralized setting, enabling the preservation of data privacy for clients. Clients maintain their private

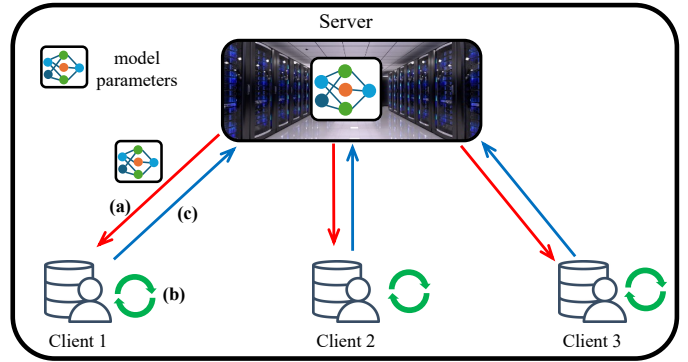


Fig. 2. **The overview of federated learning process.** (a): The server distributes a global model to clients. (b): Each client initializes the local model with the distributed one and trains a neural network using their dataset (c): Clients upload the locally trained model parameters to the server. Then, the server averages the aggregated models.

data and do not transfer sensitive information to a central server. However, data privacy causes heterogeneity problems, where clients have different data distributions, and the server can not control clients. Therefore, the trained model of each client diverges, which is a crucial factor for convergence and performance in FL. Therefore, researchers mainly have been dedicated to handling the case with a substantial heterogeneity of data across clients, resulting in the diverse strategies, including FedAvgM [17], FedProx [18], SCAFFOLD [19], FedOpt [20], FedDyn [21], and FedGF [22].

Researchers have suggested a variety of FL datasets for various tasks to establish thorough evaluation of the FL algorithms ranging from image classification [5], [23], natural language processing (NLP) [5], [24], audio emotion recognition [25], multimodal learning [26], to graph-based learning [27]. For organizing the agreed framework for the FL settings, several FL testing environments have been publicly researched and released, including Flower [28], FedML [29], FedScale [30], and FedLab [31].

Regardless of the datasets and environments, the most crucial factor in FL evaluation is demonstrating the effectiveness of methods with strong data heterogeneity across clients. When each sample contains a simple semantic, such as a single target label, unified strategies exist to impose heterogeneity across clients by diversifying the prior distribution of the target label. Specifically, two main strategies include **i**) sampling the prior distribution of each client from Dirichlet distribution [21], and **ii**) chunking per-class data samples into multiple shards, where a fixed number of shards are allocated to each client, resulting in heterogeneity between clients [32], [33].

However, when each sample bears multiple semantics, the current methods are not easily extended, so many works rely on random splits into clients, which cannot impose heterogeneity across clients. We suggest a benchmark process with well-controlled semantic heterogeneity across clients for fully evaluating deep models in FL settings with multi-semantics. One recent work has suggested a benchmark called FedNLP [24] to impose semantic heterogeneity across clients, particu-

larly in the NLP field, but it relies on the pretrained language model to discover semantic clusters and cannot be extended to vision tasks. In contrast, our benchmark does not rely on extra pretrained models and considers the first-ever developed FL panoptic scene graph generation (PSG) testing environment.

B. Panoptic Scene Graph Generation (PSG)

Scene graphs are crucial for scene understanding in computer vision tasks, representing objects (nodes), which are represented by bounding boxes or pixel-wise segmentation, and predicates (relationships, edges) in a graph structure. Predicting the bounding boxes and relationships between bounding boxes constitute scene graph generation. Recently, Conditional Random Field (CRF) [34], TransE [35], [36], CNN [37], [38], RNN/LSTM [39]–[43], GCN [44]–[46] based scene graph generation methods were studied. Subsequently, the PSG task has been proposed [47], which delves deeper into the scene graph generation by using panoptic segmentation masks instead of bounding boxes. The difference between PSG and classic scene graph generation is that PSG uses panoptic segmentation [48] masks rather than bounding boxes. The difference between the two tasks can be expressed as follows:

$$\Pr(G|I) = \Pr(B, S|I), \quad (1)$$

$$\Pr(G|I) = \Pr(M, S|I), \quad (2)$$

where $I \in \mathbb{R}^{H \times W \times 3}$ is the input image, and B and M means bounding boxes and segmented masks, respectively. S consists of the labels and their relations. And G is the scene graph. Therefore, existing scene graph generation methods can be applied to PSG tasks. Research on PSG [49]–[53] has been diverse and rapidly advancing recently.

Long-tailed Problem: The scene graph generation tasks face the long-tailed problem [54]. Positional relationships among objects constitute the majority of the predicates, leading to a visual relationship complexity of $\mathcal{O}(N^2R)$ for N objects and R predicates [16]. This exacerbates the long-tailed problem in SGG datasets, prompting various recent approaches [49]–[51], [55]–[60] have been proposed to address this issue.

To perform challenging vision tasks such as PSG, having more data typically leads to training better models. However, in reality, the photos held by different clients are unlikely to be similar, and collecting such data on the server for training poses a threat to data privacy. Despite this, there have been no attempts to apply FL to the PSG task, highlighting the necessity for this research. Furthermore, the data heterogeneity issue in FL appears similar to the long-tailed problem in the scene graph generation tasks. In addition, the long-tail problem is similarly dealt with in FL [61], [62].

III. BACKGROUND

A. Federated Learning

We briefly introduce the preliminaries of federated learning (FL) by focusing on the foundational baseline, i.e., FedAvg, [1]. FL settings contain a single server and K clients. The training process consists of iterative rounds, where the server

and clients communicate the model parameters to each other. At each round t , a server initiates the round by broadcasting a global model w^t to all clients. Each client then performs local training with its own data to obtain the locally trained model, i.e., w_k^t , where k is the client index. After that, the server aggregates the locally trained model to compute the average model, which works as the global model of the next round:

$$w^{t+1} = \sum_{k=1}^K \frac{n_k}{n} w_k^t, \quad (3)$$

where n_k is the number of data samples on client k , and n is the total data samples across all clients. Notably, our formulation assumes full participation of all clients, but it can be extended to partial participation by letting a subset of clients participate in the aggregation for each round.

B. Formalizing Heterogeneous Settings

The heterogeneity of distributed data is a critical factor for FL. When data distribution across clients is homogeneously, then the data distribution is identical for all clients, the so-called independent and identically distributed (IID) case. Otherwise, when the distribution diversifies across clients, we call it the non-IID case. We here describe the existing methods for establishing the non-IID cases in FL.

Label-based partition: Label-based data partitioning is the most widely-used approach where the dataset is distributed according to the label of samples. For instance, shard-based partitioning [1] divides the dataset into shards with each shard containing data samples of one or a few classes. Each client receives one or more shards randomly, resulting in each client owning data samples that are biased toward specific classes. Dirichlet distribution-based partitioning [21] offers a controllable and flexible method for simulating non-IID data distributions. The Dirichlet distribution is parameterized by a concentration parameter α ; as α gets close to 0, the sampled prior distribution is biased toward specific classes, in contrast, as α gets close to ∞ , the sampled prior distribution tends to be uniform over all classes.

Feature- or attribute-based partition: A feature commonly refers to an attribute of data samples. For example, when predicting an outcome based on the values from specific sensors, the location of the sensor can be its feature. In such cases, non-IID data can be constructed based on the location. The data features among clients may be completely non-overlapped, partial-overlapped, or full-overlapped [63]. Non-overlapped features refer to cases where the features in the data are different from each other. For instance, some data might include ‘gender’ and ‘age’ as features, while other data might include ‘height’ and ‘weight’. Partial-overlapped features refer to cases where the data shares some, but not all, features. For example, when taking photos of an object from the left and right sides, the images capture the same object but are not identical. Fully overlapped features refer to cases when the data features are completely identical, which is the most common scenario. Based on the degree of feature overlap, we can dynamically construct data heterogeneity.

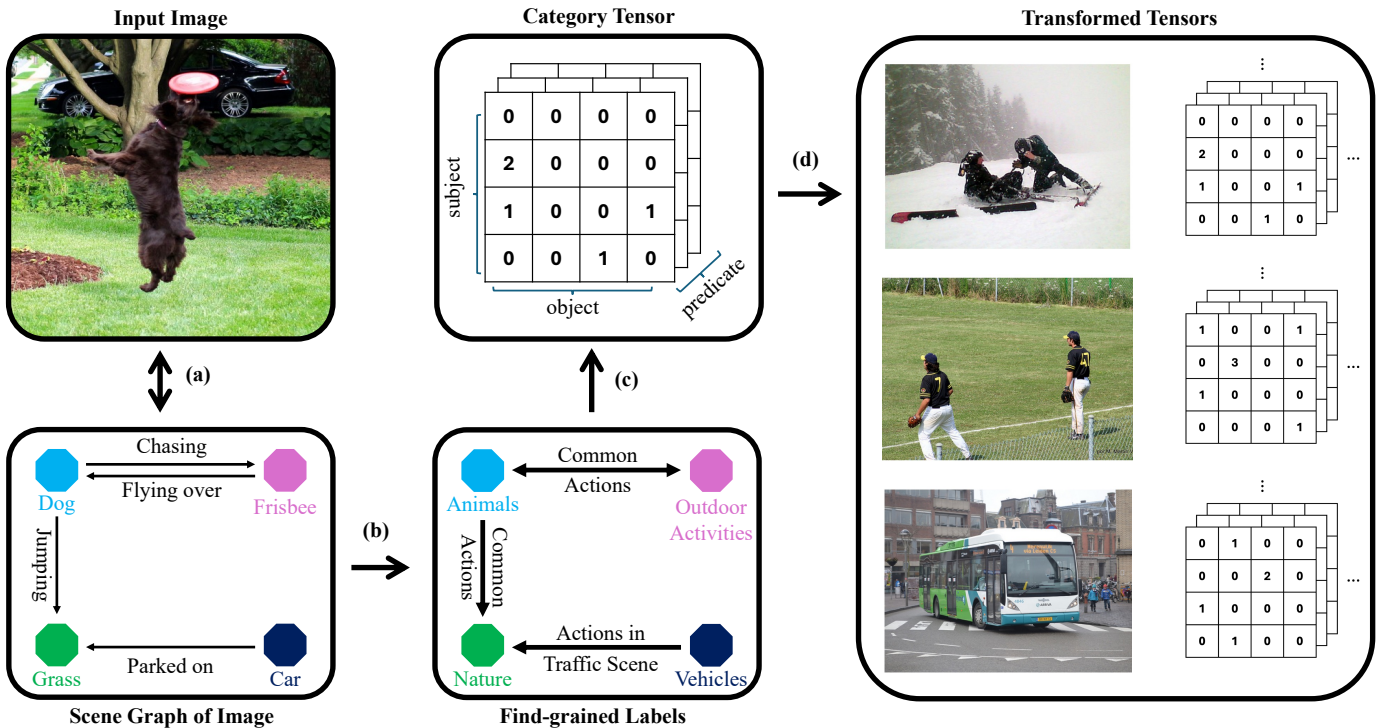


Fig. 3. **Category Tensor K-means Clustering Pipeline.** (a) We make a graph using the objects, subjects, and predicates of each image. (b) Then, we map each label into the super-classes of fine-grained labels. (c) Categorized relations (subject, object, and predicate) are converted into the category tensor. (d) We transform every input image into a category tensor and perform K-Means Clustering.

Temporal partition: Temporal partitioning leverages the temporal and spatial variability of data to construct non-IID datasets. For instance, when utilizing stock market data, data heterogeneity can be created by assigning data from specific periods to individual clients.

In brief, feature-based and temporal partitioning are strongly related to the given task or datasets, so the applicability to a wide range of FL scenarios is severely limited. Therefore, most of the works with algorithmic developments of FL rely on the label-based partitioning method.

IV. A BENCHMARK PROCESS FOR FL WITH MULTI-SEMANTIC DATASETS

For a given multi-semantic dataset, each data sample contains multiple annotations, i.e., $(x, \mathcal{Y}) \in \mathcal{D}$, where x is an input, $\mathcal{Y} = \{y_1, \dots, y_M\}$ is a multi-semantic label, M is the possible number of labels for each data sample, and \mathcal{D} represents the dataset. Here, we introduce our benchmark process to distribute the multi-semantic data samples into K multiple clients with controllable semantic heterogeneity. The key steps are twofold: i) discovering data clusters with different semantics and ii) data partitioning with controllable semantic heterogeneity across clients.

A. Discovering Data Clusters: K-means Clustering of Category Tensor

For a given multi-semantic \mathcal{Y} , we transform it to *category tensor* \mathcal{F} by allocating each label y_i into an orthogonal axis

of the tensor, i.e., $\mathcal{F}(\mathcal{Y}) \in \mathbb{R}^{N_1 \times \dots \times N_L}$, where there are N_1, \dots, N_L possible categories for each respective label of \mathcal{Y} . We then apply K -means Clustering on the collection of $\mathcal{F}(\mathcal{Y})_1^{|\mathcal{D}|}$ of overall dataset:

$$\mathcal{K}(\mathcal{F}(\mathcal{Y})_1^{|\mathcal{D}|}) \rightarrow \{\mathcal{C}_1, \dots, \mathcal{C}_n\}, \quad (4)$$

where n is the discovered number of clusters that can be determined depending on the dataset and \mathcal{C}_i indicates the collection of samples assigned to i -th cluster. With the obtained clustering, we can transform a data (x, \mathcal{Y}) into (x, \mathcal{C}) to impose the cluster label \mathcal{C} with semantic information, which is a one-hot label with 1 for the assigned cluster. Through this clustering, we can perform the label-based partition while fully utilizing the multi-semantic information of each data sample with cluster label \mathcal{C} . We present the overall pipeline to Fig 3.

B. Data Partition with Semantic Heterogeneity

We acquire n clusters from (4). It trivially raises the issue that the clusters are not evenly distributed, so the number of samples assigned to each cluster would deviate for different clusters, i.e., *cluster imbalance*. The *cluster imbalance* prevents rigorous evaluations of FL to handle semantic heterogeneity because a model becomes overfitted to dominant clusters without balanced training across different semantics. The cluster imbalance stems from the long-tailed problem, which is a key challenge in scene graph generation datasets. In other words, we have to create data heterogeneity for FL,

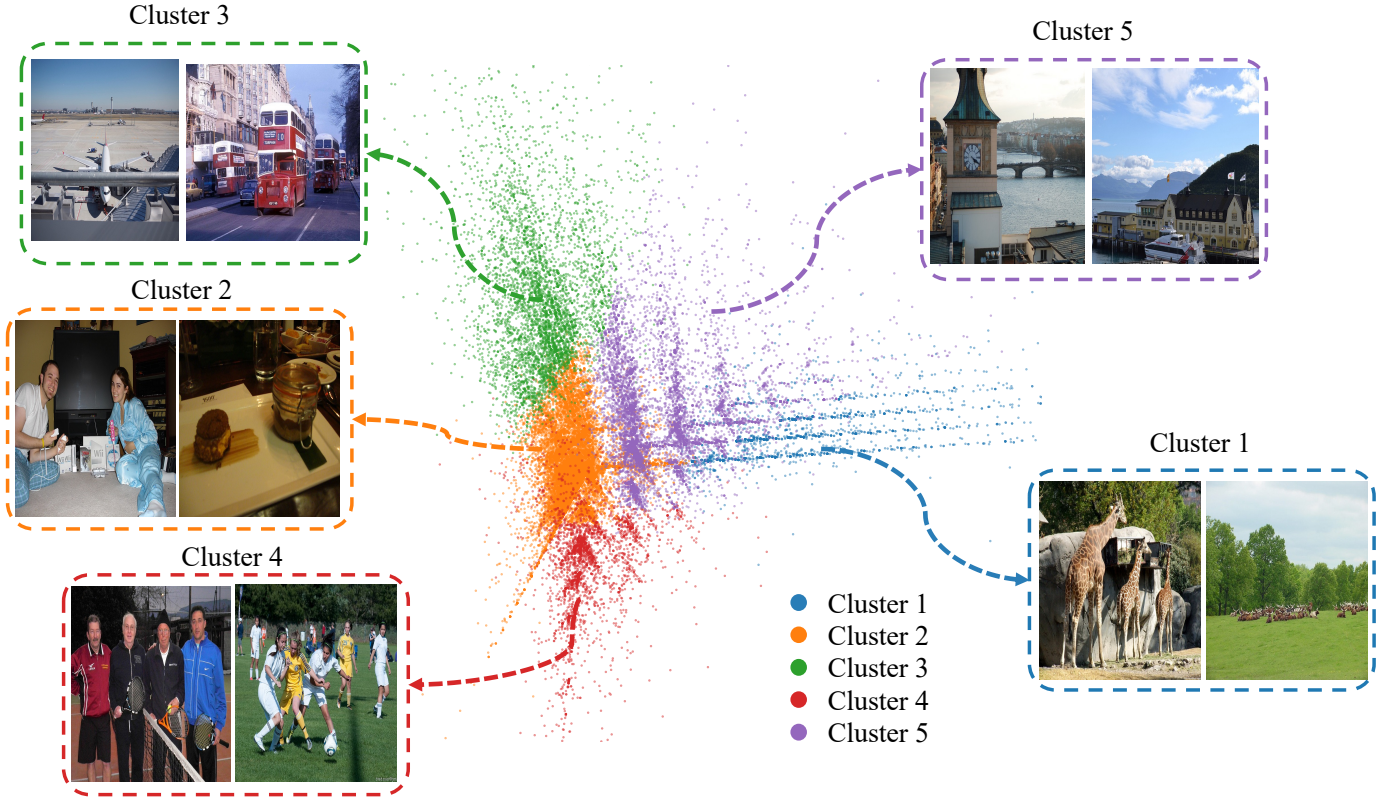


Fig. 4. Semantic clusters of PSG dataset (a visualization via Principal Component Analysis)

which makes it difficult to distinguish from the long-tailed problem. If the amount of data in each cluster is equalized, the long-tailed problem may be partially alleviated. Furthermore, considering the federated learning scenario, this cluster imbalance is likely to bias the update of the global model in the update direction of users belonging to the dominant cluster. That is, it causes overfitting to a dominant cluster, which makes it difficult to closely compare each method. Consequently, we need to equalize the data quantity of each cluster: $\hat{C}_k = \text{Sample}(\mathcal{C}_k, m)$, for all $1 \leq k \leq n$, where $m = \min_{k \in [n]} \{|\mathcal{C}_k|\}$, $|\mathcal{C}_k|$ is the cardinality of the k -th cluster \mathcal{C}_k , and $\text{Sample}(\mathcal{C}_k, m)$ denotes a function that randomly selects m data samples from cluster \mathcal{C}_k .

Now, we are ready to apply label-based partition to these clusters, enabling us to impose semantic heterogeneity. Our benchmark suggests two partition strategies as follows.

Shard-based partition: Each client chooses $p (\leq n)$ clusters. We then split each cluster into disjoint shards or chunks, where the number of shards equals the number of clients who selected the cluster. After splitting, the shards are distributed to the corresponding clients. If $p = n$, all clients are assigned to all clusters, making the data distribution homogeneous. The distribution is close to heterogeneous for smaller p values.

Dirichlet distribution-based partition: From the strategy suggested in [21], the amount of data each client takes from cluster k is governed by the sampling from the Dirichlet distribution. We can design the non-IID data partition into U

clients by sampling multinomial $\mathbf{p}_u \sim \text{Dir}_n(\boldsymbol{\alpha})$ of u -th client from Dirichlet distribution with $\boldsymbol{\alpha}$, where $\sum_{i=1}^n \mathbf{p}_{u,i} = 1$ and $\mathbf{p}_{u,i} \in [0, 1]$ for all client $u \in \{1, \dots, U\}$ and for all cluster $i \in \{1, \dots, n\}$, and $\boldsymbol{\alpha} = (\alpha_1, \alpha_2, \dots, \alpha_n)$ for all $\alpha_i \in (0, \infty]$ is a concentration parameter vector. Same as [21], we set all the element of $\boldsymbol{\alpha}$ is same, $\alpha_1 = \alpha_2 = \dots = \alpha_n$. Each client u can sample training data from a dataset according to a proportion $\mathbf{p}_{u,i}$ without replacing each cluster i . The data heterogeneity can be controlled by a value of α . As α increases, the homogeneity of the data across clients increases, while as α decreases, the heterogeneity of the data across clients increases.

C. Proof-of-concept: FL Benchmark for Panoptic Scene Graph Generation (PSG)

Herein, we provide a proof-of-concept of our FL benchmark process by constructing the FL benchmark for PSG dataset.

i) Discovering data clusters: PSG dataset contains object, subject, and predicate labels for each image sample. For simplicity, we utilize 13 object/subject categories and 7 predicate categories, which are the super-classes of fine-grained labels. Due to page limitations, we have uploaded the object/subject and predicate categories we used to our GitHub. Therefore, the dimension of the category tensor is $\mathcal{F}(\mathcal{Y}) \in \mathbb{R}^{13 \times 13 \times 7}$. For the category tensor, we perform K -means Clusters to obtain multiple semantic clusters. Consequently, we obtain 5 different

clusters with discriminated semantics:

$$\mathcal{K}(\mathcal{F}(\mathcal{Y})_1^{|\mathcal{D}|}) \rightarrow \{\mathcal{C}_1, \mathcal{C}_2, \mathcal{C}_3, \mathcal{C}_4, \mathcal{C}_5\}. \quad (5)$$

Fig. 4 illustrates the sample images from each cluster and the PCA clustering result image. By examining the samples for each cluster, we observe the following distinguished features for each cluster and the imbalance between clusters:

- **Cluster 1** (occupying 5% of datasets)
This cluster primarily contains images related to animals. We observe that it contains a large number of **animal objects** compared to others. The predicates are composed of actions that animals trivially perform.
- **Cluster 2** (occupying 58% of datasets)
This cluster is dominated by **daily photographs of people**, which constitutes the largest portion of PSG dataset. This cluster mainly contains many objects related to daily activities by human beings, such as food photographs that frequently appear in daily life.
- **Cluster 3** (occupying 11% of datasets)
This cluster mainly includes urban landscape and transportation photos, which encompass many predicates related to vehicles, such as ‘parking on’ and ‘driving (on).’
- **Cluster 4** (occupying 7% of datasets)
This cluster is composed of **sports** images. It contains many objects associated with sports and predicates such as ‘playing,’ which are more prevalent than others.
- **Cluster 5** (occupying 19% of datasets)
This cluster corresponds to **urban/nature-combined landscapes**, which typically include buildings, the sky, and a river in the images. Due to objects related to natural elements, the predicates in this cluster are predominantly positional rather than action-oriented.

Notably, Clusters 2 and 4 contain somewhat similar images, mainly of ‘people’. However, the predicates in Cluster 4 relate to sports activities, which is clearly discriminated from Cluster 2. Also, Cluster 3 and 5 look similar because of urban landscapes, but Cluster 3 leans to focus on cityscapes with transportation, and Cluster 5 focuses on urban/nature-combined city views. The qualitative visualization clearly demonstrates that our K-means Clustering of Category Tensor effectively and intuitively segments PSG dataset, leading to the splits given semantic information.

ii) Data partition: Based on the discovered 5 semantic clusters, our benchmark provides two options for data distribution: i) Shard-based partitioning and ii) Dirichlet distribution-based partitioning. Regardless of the choice of partitioning, when partitioning becomes heterogeneous, the data distribution at clients strongly deviates in the sense of semantic clusters, which leads to strong semantic heterogeneity. Otherwise, the data distribution of clients becomes homogeneous, yielding evenly distributed semantic information. The data partitioning is quite straightforward, so we will further describe the detailed settings in the following Section V.

TABLE I
DATASET INFORMATION

Data	Amount	
PSG dataset - Train	46 K	
Cluster	Balanced (24.5%)	Imbalanced (100%)
Cluster 0	2.2K (4.9%)	2.2K (4.9%)
Cluster 1	2.2K (4.9%)	27K (58.1%)
Cluster 2	2.2K (4.9%)	5.1K (10.9%)
Cluster 3	2.2K (4.9%)	3.3K (7.1%)
Cluster 4	2.2K (4.9%)	8.8K (19.0%)

V. EXPERIMENTS: BENCHMARKS FOR PSG IN FL

A. Experiment Settings

We extensively evaluate the existing panoptic scene graph generation (PSG) models on our benchmark, including the following methods: IMP [39], MOTIFS [40], VCTree [42], and GPS-Net [55]. In these PSG methods, we use the same pretrained object detector Faster R-CNN [64]. The communication cost is the crucial factor in FL scenarios; we freeze the pretrained object detector and focus on predicate classification. Therefore, each client exclusively trains and aggregates the relation head, which is responsible for processing predicates.

Dataset description: For the detailed comparison of experiments, we utilize PSG dataset [47] which includes diversified images with rich relational annotations, where each image is annotated with objects, panoptic segmentation masks, and fine-grained relationships between those objects. It not only identifies individual objects and their relationships but also includes stuff (amorphous background regions like “sky” or “grass”), which is often overlooked in other datasets. PSG dataset leverages VG150 [65] and COCO [66] datasets, which are not perfect but popularly used in scene graph generation tasks, by integrating their comprehensive object and relationship annotations into a more focused dataset designed specifically for the scene graph generation. To be specific, PSG dataset directly inherits the panoptic segmentation annotations from COCO. On the other hand, the VG150 dataset contains many ‘trivial’ (not meaningful) predicates with the direction of predicates (e.g., of in hair-‘of’-man, has in man-‘has’-head), and PSG dataset gets rid of these predicates. PSG dataset contains 133 objects and 374 relationships, sufficiently covering the diversity from the VG150 and COCO datasets while compensating for their limitations. These relationships are more detailed and extensive than in other datasets, allowing for richer scene graph representations.

The training dataset comprises 46,563 images. Table I describes the information about the dataset we have composed with Category Tensor K-means Clustering described in Fig. 3. An imbalanced dataset refers to a dataset where the number of data points in each cluster is not equal after clustering. As mentioned in Sec IV-B, to eliminate cluster imbalance, we randomly sampled the data from each cluster to match the quantity of the smallest cluster, Cluster 0. This process ensured that all clusters had the same amount of data (2.2K images), resulting in a balanced dataset.

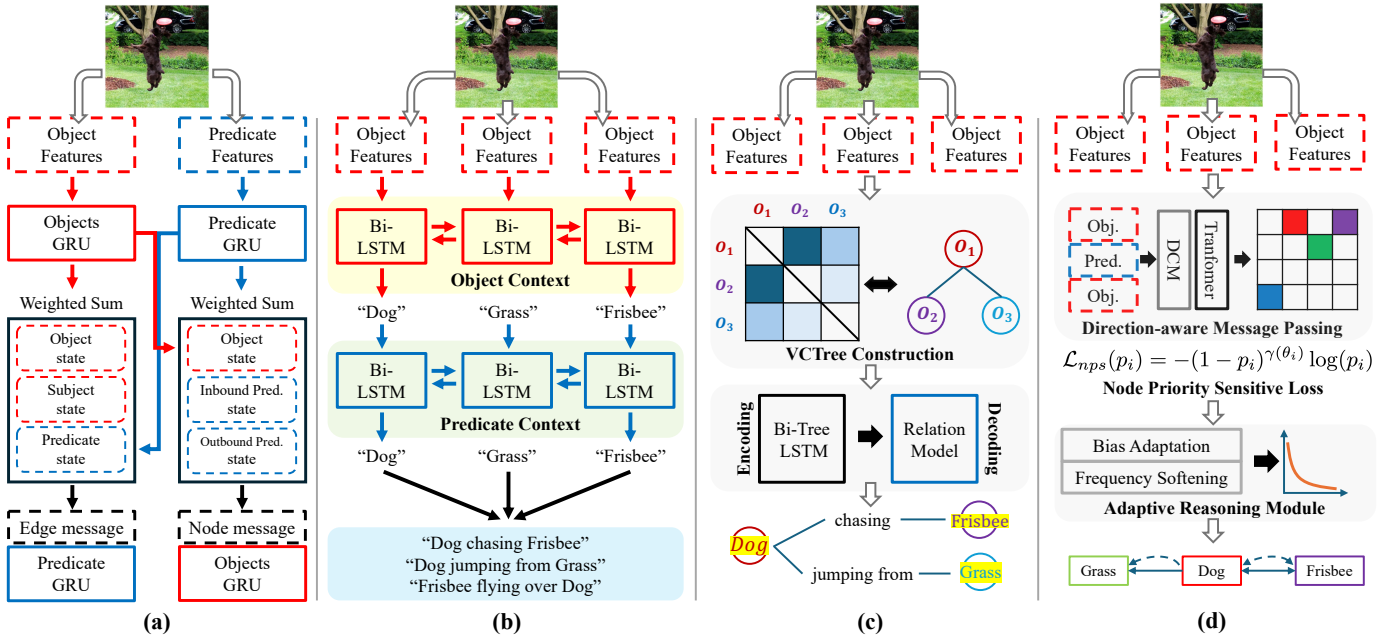


Fig. 5. Overview of PSG Methods (a) IMP, (b) MOTIFS, (c) VCTree, (d) GPS-Net.

Baseline description: We chose four panoptic scene graph generation models to validate our benchmark. For ease of understanding, we present the overview of PSG methods in Fig. 5. (a) IMP [39] (Iterative Message Passing) is a method in scene graph generation that repeatedly delivers messages for each node (object) and edge (relationships) and updates information to optimize objects and relationships simultaneously with GRUs. (b) MOTIFS [40] leverages the role of motifs in object relationships to guide scene graph generation, using bi-LSTMs to model context for better relationship prediction. (c) VCTree [42] constructs a dynamic tree structure to hierarchically capture visual and semantic dependencies among objects using the bidirectional TreeLSTM, enabling effective representation of relationships for scene graphs. (d) GPS-Net [55] enhances scene graph generation by integrating the Graph Property Sensing module that dynamically captures both global and local contextual properties of the graph. The Graph Property Sensing module consists of (1) Direction-aware Message Passing (DMP), (2) Node Priority Sensitive Loss (NPS-loss) utilizing object classification scores p_i and (3) Adaptive Reasoning Module (ARM). It leverages an adaptive message-passing mechanism to encode object relationships better and address biases in the data, resulting in more accurate and context-aware scene graphs.

Experiment setups: We set up an FL scenario with one server and 100 clients, distributing the training data of the existing PSG dataset [47] to the 100 clients. The test data for our benchmark was the same as PSG test dataset. In each round, five active clients were randomly selected, and the test data was evaluated using the aggregated global model from the server. Each client performs local training with one epoch and a batch size 16. The total number of training rounds reaches

up to 100, and we report the R/mR@K performance of the final averaged model. Following the benchmark in [47], we set the SGD optimizer to local optimizer with a learning rate of 0.02, momentum of 0.9, weight decay of 0.0001, and gradient clipping with a max L2 norm of 35.

Benchmark setups: As described in Subsection IV-B, to ease the cluster imbalance, we randomly sampled data from each cluster to ensure an equal amount of data for each cluster. We tested 6 types of data partitioning as follows:

(1) **Random**, where data is distributed randomly among all clients, ensuring nearly equal sizes for each.

(2) **Shard-based partition IID**, where we set $p = 5$, where p is the number of clusters that client sample from. As aforementioned, when p equals the number of clusters, the data from each cluster is equally distributed among 100 clients.

(3) **Shard-based partition non-IID**, where we set $p = 1$ for imposing semantic heterogeneity. Each cluster is assigned 20 clients, and all clients have the same amount of data.

(4), (5) and (6) **Dirichlet distribution-based partition** ranging from an IID case to a strong non-IID case, where we tested three different levels of semantic heterogeneity by using $\alpha = [10, 1, 0.2]$.

Metrics: By following the work of [47] that has first suggested the PSG task, we use ‘Recall@K (R@K)’ and ‘mean Recall@K (mR@K)’ as the performance metrics, which respectively calculate the triplet recall and mean recall for every predicate category, given the top K triplets from a PSG method. K varies from 20 to 100. Moreover, R@K is dominated by high-frequency relations, and mR@K assigns equal weight to all relation classes. In datasets with severe long-tailed problems, e.g., PSG dataset, mR@K can provide more meaningful insights into model performance.

TABLE II
COMPARISON OF THE PERFORMANCES OF PSG METHODS ON THE PROPOSED FL BENCHMARK

R/mR @K	Method	CL [†]	Random	Shard		Dirichlet distribution		
				IID	non-IID	$\alpha = 10 (\approx \text{IID})$	$\alpha = 1$	$\alpha = 0.2$
R/mR @20	IMP	16.54 / 6.55	12.45 / 3.08	12.62 / 3.20	11.26 / 2.28	12.31 / 3.36	12.10 / 2.92	9.31 / 1.78
	MOTIFS	<u>16.97</u> / <u>7.56</u>	<u>13.54</u> / <u>4.60</u>	<u>13.26</u> / <u>4.64</u>	<u>13.33</u> / <u>4.06</u>	<u>13.33</u> / <u>4.39</u>	<u>13.34</u> / <u>4.09</u>	<u>13.25</u> / <u>4.28</u>
	VCTree	16.80 / 7.20	12.73 / 4.38	13.00 / 4.57	12.49 / 3.99	13.00 / 4.42	12.86 / 4.36	13.06 / 4.17
	GPS-Net	18.00 / 7.83	13.93 / 5.98	14.83 / 6.90	14.57 / 5.90	14.88 / 6.33	14.82 / 6.16	14.38 / 5.91
R/mR @50	IMP	17.87 / 6.96	13.89 / 3.44	13.97 / 3.53	12.57 / 2.59	13.79 / 3.73	13.40 / 3.23	10.83 / 2.03
	MOTIFS	<u>18.59</u> / <u>8.01</u>	<u>15.07</u> / <u>5.05</u>	<u>14.82</u> / <u>5.06</u>	<u>14.92</u> / <u>4.48</u>	<u>14.77</u> / <u>4.71</u>	<u>14.63</u> / <u>4.44</u>	<u>14.77</u> / <u>4.64</u>
	VCTree	18.54 / 7.70	14.20 / 4.75	14.50 / 4.94	14.04 / 4.41	14.32 / 4.82	14.34 / 4.78	14.51 / 4.56
	GPS-Net	19.69 / 8.30	15.63 / 6.51	16.42 / 7.37	16.37 / 6.36	16.46 / 6.74	16.34 / 6.62	16.01 / 6.36
R/mR @100	IMP	18.37 / 7.11	14.46 / 3.56	14.45 / 3.65	13.06 / 2.68	14.48 / 3.89	13.92 / 3.35	11.25 / 2.10
	MOTIFS	<u>19.15</u> / <u>8.14</u>	<u>15.64</u> / <u>5.16</u>	<u>15.38</u> / <u>5.20</u>	<u>15.43</u> / <u>4.65</u>	<u>15.33</u> / <u>4.86</u>	<u>15.15</u> / <u>4.62</u>	<u>15.18</u> / <u>4.71</u>
	VCTree	19.02 / 7.82	14.69 / 4.87	14.97 / 5.05	14.62 / 4.54	14.87 / 4.97	14.90 / 4.90	15.03 / 4.68
	GPS-Net	20.28 / 8.47	16.34 / 6.66	17.08 / 7.55	16.91 / 6.49	17.10 / 6.91	16.84 / 6.77	16.55 / 6.51

[†] For centralized learning (CL) is with a centralized dataset without considering the FL settings.

Bold refers the best performance and underline denotes the 2nd performance.

B. In-depth Analysis

Our intuition is that the performance of models is expected to show the following order: Centralized learning (CL) \geq IID \geq Random \geq non-IID, when our benchmark effectively imposes semantic heterogeneity for the FL setting. The experimental results follow our intuition as well.

Results: Table II shows the test accuracy on the test set of PSG dataset. We have focused on the Mean Recall (‘mR’) performance. Also, we focus on the most challenging case with $K = 20$.

i) CL vs. IID. The performance has been mostly degraded when comparing CL and IID cases. The averaged gaps for mR@20 are -2.45% and -2.71% , for ‘Shard-IID’ and ‘Dir($\alpha = 10$)’, respectively. Each client has approximately 114 images, and due to the limited data, there appears to be a performance difference between the CL and IID scenarios. CL can collectively form a mini-batch across clients, but IID forms a mini-batch per client in a decentralized manner.

ii) IID vs. Random. When data is randomly divided, it will tend to have a distribution close to IID so that there is a minimal performance drop. The averaged gaps for mR@20 are -0.32% and -0.12% , for ‘Shard-IID’ and ‘Dir($\alpha = 10$)’, respectively. The results confirm that the random partitioning naively conducted in prior studies is unsuitable for imposing semantic heterogeneity, showing similar results as the IID case.

iii) IID vs. non-ID. We confirm large performance degradations in most cases. First, in the case of a shard-based partition, the averaged gap for mR@20 is -0.77% . Second, in the case of the Dirichlet distribution-based partition, i.e., comparing Dir($\alpha = 10$) and Dir($\alpha = 0.2$), the averaged gap for mR@20 is shown to be -0.64% . The performance drops from IID to non-IID reveal that PSG methods struggle to aggregate a global model when facing a string semantic heterogeneity. Also, when a PSG method shows a minimal performance drop due to the heterogeneity, it directly demonstrates the robustness against semantic heterogeneity. MOTIFS shows the outliers in mR, where the moderate non-IID case ($\alpha = 1$) compared to the non-IID case ($\alpha = 0.2$) shows minimal differences: 4.09%

vs. 4.28% in mR@20, and 4.62% vs. 4.71% in mR@100. Although the results may seem unexpected, the differences are not significant. Notably, when $\alpha = 10$, corresponding to the IID case, shows the best performance: 4.39% in mR@20 and 4.86% in mR@100, aligning with our expectations. Based on this observation, we conjecture that the behavior at the moderate non-IID can be a little shaky in a few cases, but it behaves as expected in the IID case.

PSG Model comparisons: We here to discuss the robustness of the existing PSG methods against semantic heterogeneity. We conclude that IMP is shown to be relatively vulnerable in handling semantic heterogeneity in FL, i.e., a large gap of -1.58% for mR@20 is observed when comparing Dir($\alpha = 10$) and Dir($\alpha = 0.2$). Compared to others, it has a relatively smaller model architecture and suffers from the long-tailed problem in PSG dataset. We conjecture that the aspects of IMP lead to considerable performance drops in our non-IID testing. VCTree includes a tree construction process trained through reinforcement learning, resulting in a more complex model structure compared to MOTIFS. Consequently, in a FL scenario with small-scale client data, the performance of VCTree is degraded. GPS-Net employs key elements, e.g., DMP, NPS-loss, ARM, to resolve the long-tailed problem. We conjecture that it yields the outperforming results of GPS-Net in our FL benchmarks. In FL, clients have a small number of data samples, which makes worse the long-tailed problem. Because GPS-Net has two key factors that pay more attention to objects and predicates with smaller occurrences, it shows remarkable performances.

C. Convergence Behavior

We present the convergence behaviors of four models on the shard and Dirichlet distribution-based partition method in Fig. 6. When we compare the non-IID and IID cases of shard, GPS-Net shows remarkable performance improvement in IID. GPS-Net has three key modules (DMP, NPS, ARM). In prior work [47], DMP was the key module for the high performance in VG150, which has the direction of predicates in the dataset

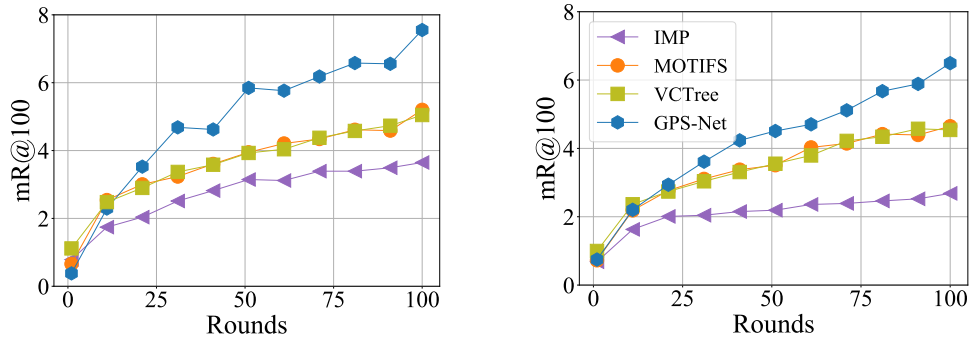


Fig. 6. Convergence behaviors of the balanced dataset for Shard IID (Left) and Shard non-IID (Right) cases

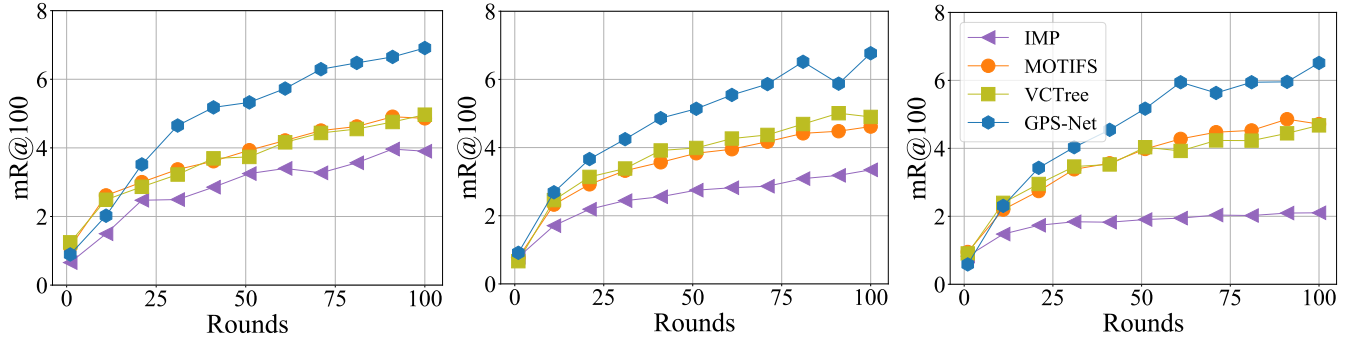


Fig. 7. Convergence behaviors of the balanced dataset for Dirichlet distribution (Left: $\alpha = 10$, Middle: $\alpha = 1$, Right: $\alpha = 0.2$)

(e.g., of in hair-of-man, has in man-has-head). Because these predicates are removed in PSG dataset, the DMP module has a lower effect on performance. However, we conjecture that other modules (NPS, ARM) designed to solve long-tailed problems are effective in the FL scenarios. As a result, the performance of GPS-Net shows the fastest convergence behavior. Despite these modules, GPS-Net shows a decrease in convergence speed under the non-IID situation. MOTIFS and VCTree show similar behaviors in IID and non-IID cases, and they also have the same model structures(LSTM) and do not consider the long-tailed problem. These two methods do not seem to be significantly affected in terms of convergence speed by the non-IID situation. IMP also showed a critical decrease in convergence speed under the non-IID situation.

We also show the convergence behavior for Dirichlet distribution in Fig. 7, where α is the [10, 1, 0.2]. It shows similar results to behaviors of the shard-based partition scenario. Overall, as the data heterogeneity increases, the convergence behaviors show decreased performance. However, MOTIFS and VCTREE still do not seem to be significantly affected in terms of convergence speed in both Shard-based partition and Dirichlet distribution-based partition.

D. Various FL Scenarios

In this section, we conduct a series of experiments to investigate the impact of different factors on federated learning performance. Federated learning operates in diverse environments, making it essential to test various scenarios to better understand how the approach performs. By manipulating key

TABLE III
COMPARISON OF PERFORMANCES FOR THE NUMBER OF TOTAL CLIENTS.

R/mR@100	Method	Shard IID	Shard non-IID
Clients 50	IMP	15.62 / 4.60	14.92 / 4.70
	MOTIFS	18.24 / 7.74	18.22 / 6.88
	VCTree	16.61 / 6.51	16.89 / 6.40
	GPS-Net	18.54 / 7.22	18.11 / 7.29
Clients 100	IMP	14.45 / 3.65	13.06 / 2.68
	MOTIFS	15.38 / 5.20	15.43 / 4.65
	VCTree	14.97 / 5.05	14.62 / 4.54
	GPS-Net	17.08 / 7.55	16.91 / 6.49
Clients 200	IMP	12.80 / 3.00	12.37 / 2.30
	MOTIFS	15.22 / 5.23	15.43 / 5.08
	VCTree	12.54 / 3.56	12.4 / 3.33
	GPS-Net	13.69 / 5.22	13.49 / 5.09

parameters such as the total number of clients, participation rates, and federated learning algorithms, we provide a comprehensive analysis of their effects on overall performance.

Total clients: We evaluate performances to examine the effect of number of total clients, i.e., 50, 100, and 200, in Table III. For the case of 50 clients, each client has twice as much data per client compared to the 100 clients case. Performance improves as the number of data samples that the clients have increased. Notably, VCTree shows a $2\times$ larger mR@K for 50 clients compared to 200 clients in the Shard non-IID case, indicating that VCTree is highly sensitive to the number of data samples, a critical factor in FL settings. In contrast, MOTIFS and GPS-Net are less affected by the number of data samples, with GPS-Net achieving an mR@K

TABLE IV
COMPARISON OF PERFORMANCES FOR PARTICIPATION RATES

R/mR@100	Method	Shard IID	Shard non-IID
# of clients 5	IMP	14.45 / 3.65	13.06 / 2.68
	MOTIFS	15.38 / 5.20	15.43 / 4.65
	VCTree	14.97 / 5.05	14.62 / 4.54
	GPS-Net	17.08 / 7.55	16.91 / 6.49
# of clients 20	IMP	13.91 / 3.25	15.31 / 4.04
	MOTIFS	17.3 / 6.39	16.83 / 6.23
	VCTree	15.03 / 4.83	14.92 / 4.73
	GPS-Net	16.81 / 6.36	16.66 / 6.04

TABLE V
COMPARISON OF THE COMMUNICATION COST FOR HETEROGENEITY

Method	# of model parameters	Shard IID	Shard non-IID
IMP	32M	64(x 1)	64(x 1)
MOTIFS	63M	63(x 0.98)	63(x 0.98)
VCTree	59M	59(x 0.92)	59(x 0.92)
GPS-Net	37M	37(x 0.57)	37(x 0.57)

greater than 5.09 and MOTIFS exceeding 4.65, significantly outperforming both IMP and VCTree across all cases.

Participation rates: We also evaluate the performance according to the number of participating clients, i.e., 5 and 20, in Table IV. As the number of participants increased, the performance of MOTIFS improved remarkably. According to previous FL studies, mainly handled the image classification task, increasing participation rate leads to improved performance in FL environments. However, in the PSG task, as the number of users increases, the performance does not show similar behaviors without MOTIFS. In other words, rather than increasing the number of participants in each round, a larger amount of data for each participant can result in greater performance improvement in this task.

Additionally, we have to focus on the performances of IMP in various FL scenarios. IMP is the oldest method in our experiments and shows a lower performance in the experiments of existing studies [42], [47]. Therefore, the performance seems poor before being affected by data heterogeneity, making a detailed comparison difficult.

E. Analysis of Communication Cost

Communication efficiency is one of the most important factors because communication costs are crucial in a practical FL scenario. When thinking of communication rate, as in a scenario with limited communication resources, we compare the methods by rigorously measuring the actual communication costs required to reach the same level of performance.

From the convergence behavior in Fig. 6 and 7, we compute the required communication costs to compare the communication efficiency of each method. Specifically, we calculate the total communication cost, i.e., the number of model parameters multiplied by the communication round, to reach the ‘mR@100 = 2’ (the reason for the target performance is that the IMP shows the worst performance and converges near 2). We show the number of model parameters for each method and the resulting communication costs required in Table V.

TABLE VI
COMPARISON OF THE PERFORMANCES ON THE IMBALANCED DATASET

R/mR @K	Method	Shard			
		CL [47]	Random	IID	non-IID
R/mR @20	IMP	16.5 / 6.52	16.10 / 5.68	16.38 / 5.97	15.50 / 4.75
	MOTIFS	20.0 / 9.10	16.66 / 6.52	16.64 / 6.60	16.34 / 6.32
	VCTree	20.6 / 9.70	16.49 / 6.42	16.93 / 7.03	16.46 / 6.09
	GPS-Net	17.8 / 7.03	17.90 / 7.29	18.12 / 7.38	17.98 / 8.10
R/mR @50	IMP	18.2 / 7.05	17.53 / 6.10	17.74 / 6.43	16.89 / 5.11
	MOTIFS	21.7 / 9.57	18.26 / 7.03	18.38 / 7.12	17.89 / 6.70
	VCTree	22.1 / 10.2	17.94 / 6.84	18.47 / 7.44	17.97 / 6.52
	GPS-Net	19.6 / 7.49	19.44 / 7.77	19.78 / 7.85	19.36 / 8.46
R/mR @100	IMP	18.6 / 7.23	18.09 / 6.28	18.20 / 6.58	17.26 / 5.22
	MOTIFS	22.0 / 9.69	18.75 / 7.23	18.88 / 7.23	18.39 / 6.83
	VCTree	22.5 / 10.2	18.52 / 7.00	18.92 / 7.56	18.47 / 6.64
	GPS-Net	20.1 / 7.67	19.89 / 7.86	20.14 / 7.94	19.83 / 8.62

IMP has the smallest number of model parameters but the highest communication cost. In contrast, GPS-Net has a similar number of model parameters with IMP, which accounts for half of the total communication cost, denoting that GPS-Net is the resource-efficient scene graph generation method in FL. GPS-Net shows remarkable performance because it has core strategies to resolve the long-tailed problem. We conjecture that it shows the rapid convergence behavior to higher accuracies with fewer communication costs.

F. Cluster Imbalance Effect

Benchmark setups: To observe the effects of cluster imbalance, we do not equalize the number of data points. We tested 3 types of data partitioning as follows:

(1) **Random:** data is distributed randomly among all clients, ensuring nearly equal sizes for each.

(2) **Shard-based partition IID:** We set $p = 5$, where p is the number of clusters that client sample from. As aforementioned, when p equals the number of clusters, the data from each cluster is equally distributed among 100 clients.

(3) **Shard-based partition non-IID:** We set $p = 1$ for imposing semantic heterogeneity. This time, clients are allocated to each cluster based on the amount of data in each cluster rather than assigning an equal number of clients to all clusters.

Results: The results in Table VI differ in some aspects from the analysis in the main paper. Firstly, the performance of all methods in FL scenarios has significantly increased. This is because the quantity of data assigned to each client has greatly increased, and models are overfitted to the dominant cluster. The performance trends of each method have changed as follows: In the case of IMP, the performance gap between CL and IID has significantly narrowed. While the performance in FL scenarios has greatly improved, the performance of CL has remained unchanged. This indicates that IMP is relatively less affected by the amount of data. In the case of MOTIFS and VCTree, the performance trends were almost similar to those observed in the previous experiments on the balanced dataset. VCTree still appears to be slightly more vulnerable to data heterogeneity compared to MOTIFS. These methods, i.e., IMP, MOTIFS, and VCTree, show that performance decreases as data heterogeneity increases. In contrast, the trends observed for GPS-Net were completely

TABLE VII
COMPARISON OF THE FEDAVG AND FEDAVGM PERFORMANCES OF PSG METHODS.

R/mR@K	Method	FedAvg Shard non-IID	FedAvgM [17] Shard non-IID	FedAdam [20] Shard non-IID
R/mR@20	IMP	11.26 / 2.28	13.23 / 3.83 (+1.55%)	13.32 / 4.78 (+2.50%)
	MOTIFS	13.33 / 4.06	15.47 / 5.80 (+1.74%)	15.89 / 5.56 (+1.50%)
	VCTree	12.49 / 3.99	15.39 / 5.66 (+1.67%)	15.53 / 5.09 (+1.10%)
	GPS-Net	14.57 / 5.90	16.18 / 5.91 (+0.01%)	15.66 / 5.98 (+0.08%)
R/mR@50	IMP	12.57 / 2.59	14.73 / 4.24 (+1.65%)	15.03 / 5.41 (+2.82%)
	MOTIFS	14.92 / 4.48	17.23 / 6.23 (+1.75%)	17.66 / 6.01 (+1.53%)
	VCTree	14.04 / 4.41	17.02 / 6.10 (+1.69%)	16.95 / 5.40 (+0.99%)
	GPS-Net	16.37 / 6.36	18.00 / 6.33 (-0.03%)	17.31 / 6.42 (+0.06%)
R/mR@100	IMP	13.06 / 2.68	15.32 / 4.38 (+1.70%)	15.63 / 5.57 (+2.89%)
	MOTIFS	15.43 / 4.65	17.83 / 6.38 (+1.73%)	18.21 / 6.14 (+1.49%)
	VCTree	14.62 / 4.54	17.58 / 6.30 (+1.76%)	17.42 / 5.53 (+0.99%)
	GPS-Net	16.91 / 6.49	18.68 / 6.52 (-0.03%)	17.90 / 6.55 (+0.06%)

(·) indicates the difference in mR@K when each algorithm is applied compared to FedAvg.

different from what was expected generally in FL scenarios. The performance reported in the previous study [47] is lower than the performance on the balanced dataset. Prior research mentioned that the key point of GPS-Net explicitly models the direction of predicates, which is why it does not perform well on PSG dataset. However, when examining the results in our main table, modeling the direction of predicates might not be the cause. Furthermore, GPS-Net showed the best results in the non-IID scenario. This is unusual and significantly deviated from our expectations. Therefore, we concluded that GPS-Net performs well when clients have sufficient data and a relatively small number of categories. Additionally, we believe that a detailed performance comparison through FL on the SGG task, rather than PSG task, would allow for a more in-depth analysis.

VI. EXTENSION TO FL ALGORITHMS

From Table II, we confirm that the improvements in PSG methods remain effective in the FL scenario. Subsequently, it is necessary to verify whether the improvements in FL algorithms are also valid within our benchmark. We conducted additional experiments on two FL algorithms that leverage momentum. Momentum-based update strategies are expected to be effective in maintaining local training closer to the global update direction. By mitigating the adverse effects of data distribution discrepancies, these algorithms can potentially enhance both convergence stability and model performance in such challenging settings.

A. FedAvgM

We present the result of applying FedAvgM [17] in Table VII. FedAvgM utilizes the momentum in updating a global model on the server side and relieves the varying directions of local updates due to the stochastic variance across clients. FedAvgM updates the global model as follows:

$$w_g^{r+1} = w_g^r - v^r, \quad (6)$$

$$v^r = \beta v^{r-1} + \sum_{k=1}^K \frac{n_k}{n} \Delta w_k^r \quad (7)$$

where β is the momentum hyperparameter for FedAvgM, n_k is the number of examples, Δw_k^r is the weight update from k 's client, and $n = \sum_{k=1}^K n_k$.

Results: FedAvgM sufficiently improves the performance of all methods. For R/mR@20, R/mR@50, and R/mR@100, there are average performance improvements of +1.24%, +1.27%, and +1.30% in the Shard-nonIID case, respectively. These performance improvements under FedAvgM can be attributed to FedAvgM's momentum-based updates which help stabilize training by reducing local update oscillations in the optimization process, leading to faster convergence and better generalization across heterogeneous client data. IMP, MOTIFS, and VCTree showed noticeable performance increases, while GPS-Net did not. The performance of GPS-Net in the Shard non-IID case shows a negligible gap (i.e., $\leq 0.03\%$), indicating that GPS-Net already incorporates factors that mitigate the effects of heterogeneity.

B. FedAdam

FedOpt [20] provides a flexible framework for improving optimization in FL, enabling the use of advanced server-side optimization algorithms (e.g., AdaGrad, Adam) to improve convergence and stability. This approach effectively deals with various client data distribution differences and fluctuations in client participation rates. FedOpt uses different optimizers in local updates and global updates. In our case, we utilize the Adam [67] optimizer for global updates:

$$m^{r+1} = \beta_1 m^r + (1 - \beta_1) \Delta w^r, \quad (8)$$

$$v^{r+1} = \beta_2 v^r + (1 - \beta_2) (\Delta w^r)^2, \quad (9)$$

$$w_g^{r+1} = w_g^r - \eta \frac{m^{r+1}}{\sqrt{v^{r+1}} + \epsilon}, \quad (10)$$

where β_1 and β_2 are the momentum hyperparameters, ϵ is a small constant added to the denominator to ensure numerical stability and prevent division by 0. We present the result of applying FedAdam in Table VII.

Results: FedAdam demonstrated a marginally superior performance improvement compared to FedAvgM. For R/mR@20, R/mR@50, and R/mR@100, there are average

performance improvements of +1.30%, +1.35%, and +1.36% in the Shard-nonIID case, respectively. Interestingly, FedAdam shows a noticeable performance improvement when combined with IMP, as shown in the table. IMP has a lower initial performance (based on R/mR@20, R/mR@50, and R/mR@100) when compared to other methods (MOTIFS, VCTree, GPS-Net). However, when combined with FedAdam, it showed the greatest performance improvement (+2.89% in R/mR@100 case). IMP simply learns by iteratively updating relationships between objects. As a result, IMP is prone to learning by being overly head-class-biased in class imbalances, and performance degradation is inevitable in tail classes. In this environment, FedAdam has most likely improved its model effectively in the tail class, where losses are concentrated due to the long-tailed problem. Contrary to IMP, GPS-Net has various strategies to solve the long-tailed problem. Similar to the FedAvgM experimental result, GPS-Net showed no significant change in performance.

From these results, we can conclude that the enhancement of FL algorithms is effective when dealing with scenarios involving diverse semantic information across clients. Furthermore, the experimental outcomes with IMP and GPS-Net reveal an intriguing connection: the long-tailed problem encountered in scene graph generation tasks shares notable similarities with the data heterogeneity issues faced in FL. In scenarios where scene graph generation tasks must be addressed in a distributed data environment, selecting a scene graph generation method with a strong strategy for handling long-tailed problems or choosing an FL algorithm that effectively deals with data heterogeneity would significantly increase the likelihood of simultaneously tackling both challenges.

VII. DISCUSSION: WHY FL BENCHMARKS FOR SCENE UNDERSTANDING IS REQUIRED

In this section, we discuss the necessity and potential extensions of our benchmarks. In the media industry, companies are increasingly focused on protecting the copyrights of their original content. As a result, they have been reluctant to share raw media data externally. At the same time, there is a growing demand for leveraging AI in the media production process. Given this context, there is a pressing need for a model that can effectively learn from media content while preserving copyright. To fulfill this need, we proposed the FL scenario that allows for AI training without requiring the exposure of raw data. We believe this approach aligns well with the concept of protecting media content copyrights. Among the various tasks that utilize publicly available benchmark datasets, PSG plays a crucial role in understanding the context of media content. Scene graphs represent the relationships between objects, thus extracting the semantic meaning of the content.

This study offers a new direction for FL research, demonstrating its potential to support complex semantic learning tasks while preserving data privacy. The findings are particularly relevant for applications in sensitive domains such as healthcare and media, where privacy concerns limit centralized data sharing. Future work could extend the proposed

benchmark to diverse vision and multimodal datasets, further enhancing its generalization and utility.

VIII. CONCLUSION

This study introduces an innovative benchmark for evaluating FL algorithms on complex semantic datasets in the computer vision domain, particularly in the scene graph generation tasks. The proposed benchmark leverages semantic-based data clustering and controlled data partitioning to systematically manage semantic heterogeneity across clients, providing the first-ever FL benchmark for the PSG task.

The experimental results demonstrate that the benchmark effectively simulates the data heterogeneity, revealing critical insights into the performance of various PSG and FL algorithms under different scenarios. Notably, GPS-Net showcased remarkable robustness in FL settings, while simpler methods like IMP suffered significant performance degradation due to semantic heterogeneity. These findings underline the importance of addressing data heterogeneity in vision tasks and highlight the role of FL algorithms in enabling robust and decentralized training for complex tasks.

Furthermore, experiments with advanced FL algorithms, such as FedAvgM and FedAdam, revealed their effectiveness in mitigating data heterogeneity issues and improving model performance in FL scenarios. FedAdam, in particular, excelled at addressing the challenges posed by long-tailed data distributions, yielding substantial improvements for simpler methods like IMP. Conversely, GPS-Net exhibited minimal performance gains with these FL algorithms, reflecting its inherent robustness against data heterogeneity in design. These results emphasize the importance of selecting FL and PSG methods with complementary strengths to handle both semantic complexity and data heterogeneity effectively.

ACKNOWLEDGMENTS

This work was supported by Institute of Information & communications Technology Planning & Evaluation (IITP) grant funded by the Korea government(MSIT) (No.2021-0-00852, Development of Intelligent Media Attributes Extraction and Sharing Technology), (No. RS2020-II201336, Artificial Intelligence Graduate School Program (UNIST)), and (No. IITP-2024-RS-2022-00156361, Innovative Human Resource Development for Local Intellectualization program), and the National Research Foundation of Korea (NRF) grant funded by the Korea government (MSIT) (No. RS-2024-00459023).

REFERENCES

- [1] B. McMahan, E. Moore, D. Ramage, S. Hampson, and B. A. y Arcas, "Communication-efficient learning of deep networks from decentralized data," in *Artificial intelligence and statistics*. PMLR, 2017, pp. 1273–1282.
- [2] L. Deng, "The mnist database of handwritten digit images for machine learning research," *IEEE Signal Processing Magazine*, vol. 29, no. 6, pp. 141–142, 2012.
- [3] A. Krizhevsky, V. Nair, and G. Hinton, "Cifar-10 (canadian institute for advanced research)," 2019.
- [4] Z. Liu, P. Luo, X. Wang, and X. Tang, "Deep learning face attributes in the wild," in *Proceedings of International Conference on Computer Vision (ICCV)*, December 2015.

- [5] S. Caldas, S. M. K. Duddu, P. Wu, T. Li, J. Konečný, H. B. McMahan, V. Smith, and A. Talwalkar, "Leaf: A benchmark for federated settings," *arXiv preprint arXiv:1812.01097*, 2018.
- [6] X. Li, K. Huang, W. Yang, S. Wang, and Z. Zhang, "On the convergence of fedavg on non-iid data," *arXiv preprint arXiv:1907.02189*, 2019.
- [7] M. Yurochkin, M. Agarwal, S. Ghosh, K. Greenewald, N. Hoang, and Y. Khazaeni, "Bayesian nonparametric federated learning of neural networks," in *International conference on machine learning*. PMLR, 2019, pp. 7252–7261.
- [8] H. Wang, M. Yurochkin, Y. Sun, D. Papailiopoulos, and Y. Khazaeni, "Federated learning with matched averaging," *arXiv preprint arXiv:2002.06440*, 2020.
- [9] R. Rombach, A. Blattmann, D. Lorenz, P. Esser, and B. Ommer, "High-resolution image synthesis with latent diffusion models," in *Proceedings of the IEEE/CVF conference on computer vision and pattern recognition*, 2022, pp. 10684–10695.
- [10] A. Ramesh, M. Pavlov, G. Goh, S. Gray, C. Voss, A. Radford, M. Chen, and I. Sutskever, "Zero-shot text-to-image generation," in *International conference on machine learning*. Pmlr, 2021, pp. 8821–8831.
- [11] A. Gordo, J. Almazan, J. Revaud, and D. Larlus, "End-to-end learning of deep visual representations for image retrieval," *International Journal of Computer Vision*, vol. 124, no. 2, pp. 237–254, 2017.
- [12] A. Gordo and D. Larlus, "Beyond instance-level image retrieval: Leveraging captions to learn a global visual representation for semantic retrieval," in *Proceedings of the IEEE conference on computer vision and pattern recognition*, 2017, pp. 6589–6598.
- [13] F. Radenović, A. Iscen, G. Tolias, Y. Avrithis, and O. Chum, "Revisiting oxford and paris: Large-scale image retrieval benchmarking," in *Proceedings of the IEEE Conference on Computer Vision and Pattern Recognition (CVPR)*, June 2018.
- [14] S. Antol, A. Agrawal, J. Lu, M. Mitchell, D. Batra, C. L. Zitnick, and D. Parikh, "Vqa: Visual question answering," in *Proceedings of the IEEE international conference on computer vision*, 2015, pp. 2425–2433.
- [15] J.-B. Alayrac, J. Donahue, P. Luc, A. Miech, I. Barr, Y. Hasson, K. Lenc, A. Mensch, K. Millican, M. Reynolds *et al.*, "Flamingo: a visual language model for few-shot learning," *Advances in neural information processing systems*, vol. 35, pp. 23716–23736, 2022.
- [16] X. Chang, P. Ren, P. Xu, Z. Li, X. Chen, and A. Hauptmann, "Scene graphs: A survey of generations and applications," *arXiv preprint arXiv:2104.01111*, vol. 2, 2021.
- [17] T.-M. H. Hsu, H. Qi, and M. Brown, "Measuring the effects of non-identical data distribution for federated visual classification," *arXiv preprint arXiv:1909.06335*, 2019.
- [18] T. Li, A. K. Sahu, M. Zaheer, M. Sanjabi, A. Talwalkar, and V. Smith, "Federated optimization in heterogeneous networks," *Proceedings of Machine learning and systems*, vol. 2, pp. 429–450, 2020.
- [19] S. P. Karimireddy, S. Kale, M. Mohri, S. Reddi, S. Stich, and A. T. Suresh, "Scaffold: Stochastic controlled averaging for federated learning," in *International conference on machine learning*. PMLR, 2020, pp. 5132–5143.
- [20] S. Reddi, Z. Charles, M. Zaheer, Z. Garrett, K. Rush, J. Konečný, S. Kumar, and H. B. McMahan, "Adaptive federated optimization," *arXiv preprint arXiv:2003.00295*, 2020.
- [21] D. A. E. Acar, Y. Zhao, R. M. Navarro, M. Mattina, P. N. Whatmough, and V. Saligrama, "Federated learning based on dynamic regularization," *arXiv preprint arXiv:2111.04263*, 2021.
- [22] T. Lee and S. W. Yoon, "Rethinking the flat minima searching in federated learning," in *Forty-first International Conference on Machine Learning*, 2024.
- [23] Q. Li, Y. Diao, Q. Chen, and B. He, "Federated learning on non-iid data silos: An experimental study," in *2022 IEEE 38th international conference on data engineering (ICDE)*. IEEE, 2022, pp. 965–978.
- [24] B. Y. Lin, C. He, Z. Zeng, H. Wang, Y. Huang, C. Dupuy, R. Gupta, M. Soltanolkotabi, X. Ren, and S. Avestimehr, "Fednlp: Benchmarking federated learning methods for natural language processing tasks," *arXiv preprint arXiv:2104.08815*, 2021.
- [25] T. Zhang, T. Feng, S. Alam, S. Lee, M. Zhang, S. S. Narayanan, and S. Avestimehr, "Fedaudio: A federated learning benchmark for audio tasks," in *ICASSP 2023-2023 IEEE International Conference on Acoustics, Speech and Signal Processing (ICASSP)*. IEEE, 2023, pp. 1–5.
- [26] T. Feng, D. Bose, T. Zhang, R. Hebbar, A. Ramakrishna, R. Gupta, M. Zhang, S. Avestimehr, and S. Narayanan, "Fedmultimodal: A benchmark for multimodal federated learning," in *Proceedings of the 29th ACM SIGKDD Conference on Knowledge Discovery and Data Mining*, 2023, pp. 4035–4045.
- [27] Z. Wang, W. Kuang, Y. Xie, L. Yao, Y. Li, B. Ding, and J. Zhou, "Federatedscope-gnn: Towards a unified, comprehensive and efficient package for federated graph learning," in *Proceedings of the 28th ACM SIGKDD Conference on Knowledge Discovery and Data Mining*, 2022, pp. 4110–4120.
- [28] D. J. Beutel, T. Topal, A. Mathur, X. Qiu, J. Fernandez-Marques, Y. Gao, L. Sani, K. H. Li, T. Parcollet, P. P. B. de Gusmão *et al.*, "Flower: A friendly federated learning research framework," *arXiv preprint arXiv:2007.14390*, 2020.
- [29] C. He, S. Li, J. So, X. Zeng, M. Zhang, H. Wang, X. Wang, P. Vepakomma, A. Singh, H. Qiu *et al.*, "Fedml: A research library and benchmark for federated machine learning," *arXiv preprint arXiv:2007.13518*, 2020.
- [30] F. Lai, Y. Dai, S. S. Singapuram, J. Liu, X. Zhu, H. V. Madhyastha, and M. Chowdhury, "Fedscale: Benchmarking model and system performance of federated learning at scale," in *International Conference on Machine Learning (ICML)*, 2022.
- [31] X. H. Dun Zeng, Siqi Liang and Z. Xu, "Fedlab: A flexible federated learning framework," *arXiv preprint arXiv:2107.11621*, 2021.
- [32] I. Achituve, A. Shamsian, A. Navon, G. Chechik, and E. Fetaya, "Personalized federated learning with gaussian processes," *Advances in Neural Information Processing Systems*, vol. 34, pp. 8392–8406, 2021.
- [33] J. H. Lim, S. Ha, and S. W. Yoon, "Metavers: Meta-learned versatile representations for personalized federated learning," in *Proceedings of the IEEE/CVF Winter Conference on Applications of Computer Vision*, 2024, pp. 2587–2596.
- [34] W. Cong, W. Wang, and W.-C. Lee, "Scene graph generation via conditional random fields," *arXiv preprint arXiv:1811.08075*, 2018.
- [35] H. Zhang, Z. Kyaw, S.-F. Chang, and T.-S. Chua, "Visual translation embedding network for visual relation detection," in *Proceedings of the IEEE conference on computer vision and pattern recognition*, 2017, pp. 5532–5540.
- [36] Z.-S. Hung, A. Mallya, and S. Lazebnik, "Contextual translation embedding for visual relationship detection and scene graph generation," *IEEE transactions on pattern analysis and machine intelligence*, vol. 43, no. 11, pp. 3820–3832, 2020.
- [37] S. Woo, D. Kim, D. Cho, and I. S. Kweon, "Linknet: Relational embedding for scene graph," *Advances in neural information processing systems*, vol. 31, 2018.
- [38] G. Yin, L. Sheng, B. Liu, N. Yu, X. Wang, J. Shao, and C. C. Loy, "Zoom-net: Mining deep feature interactions for visual relationship recognition," in *Proceedings of the European conference on computer vision (ECCV)*, 2018, pp. 322–338.
- [39] D. Xu, Y. Zhu, C. B. Choy, and L. Fei-Fei, "Scene graph generation by iterative message passing," in *Proceedings of the IEEE conference on computer vision and pattern recognition*, 2017, pp. 5410–5419.
- [40] R. Zellers, M. Yatskar, S. Thomson, and Y. Choi, "Neural motifs: Scene graph parsing with global context," in *Proceedings of the IEEE conference on computer vision and pattern recognition*, 2018, pp. 5831–5840.
- [41] Y. Li, W. Ouyang, B. Zhou, J. Shi, C. Zhang, and X. Wang, "Factorizable net: an efficient subgraph-based framework for scene graph generation," in *Proceedings of the European Conference on Computer Vision (ECCV)*, 2018, pp. 335–351.
- [42] K. Tang, H. Zhang, B. Wu, W. Luo, and W. Liu, "Learning to compose dynamic tree structures for visual contexts," in *Proceedings of the IEEE/CVF conference on computer vision and pattern recognition*, 2019, pp. 6619–6628.
- [43] W. Wang, R. Wang, S. Shan, and X. Chen, "Sketching image gist: Human-mimetic hierarchical scene graph generation," in *European conference on computer vision*. Springer, 2020, pp. 222–239.
- [44] R. Herzig, M. Raboh, G. Chechik, J. Berant, and A. Globerson, "Mapping images to scene graphs with permutation-invariant structured prediction," *Advances in Neural Information Processing Systems*, vol. 31, 2018.
- [45] M. Qi, W. Li, Z. Yang, Y. Wang, and J. Luo, "Attentive relational networks for mapping images to scene graphs," in *Proceedings of the IEEE/CVF Conference on Computer Vision and Pattern Recognition*, 2019, pp. 3957–3966.
- [46] J. Yang, J. Lu, S. Lee, D. Batra, and D. Parikh, "Graph r-cnn for scene graph generation," in *Proceedings of the European conference on computer vision (ECCV)*, 2018, pp. 670–685.

- [47] J. Yang, Y. Z. Ang, Z. Guo, K. Zhou, W. Zhang, and Z. Liu, "Panoptic scene graph generation," in *European Conference on Computer Vision*. Springer, 2022, pp. 178–196.
- [48] A. Kirillov, K. He, R. Girshick, C. Rother, and P. Dollár, "Panoptic segmentation," in *Proceedings of the IEEE/CVF conference on computer vision and pattern recognition*, 2019, pp. 9404–9413.
- [49] Z. Zhou, M. Shi, and H. Caesar, "Vlprompt: Vision-language prompting for panoptic scene graph generation," *arXiv preprint arXiv:2311.16492*, 2023.
- [50] —, "Hilo: Exploiting high low frequency relations for unbiased panoptic scene graph generation," in *Proceedings of the IEEE/CVF International Conference on Computer Vision*, 2023, pp. 21 637–21 648.
- [51] L. Li, W. Ji, Y. Wu, M. Li, Y. Qin, L. Wei, and R. Zimmermann, "Panoptic scene graph generation with semantics-prototype learning," in *Proceedings of the AAAI Conference on Artificial Intelligence*, vol. 38, no. 4, 2024, pp. 3145–3153.
- [52] J. Wang, Z. Wen, X. Li, Z. Guo, J. Yang, and Z. Liu, "Pair then relation: Pair-net for panoptic scene graph generation," *arXiv preprint arXiv:2307.08699*, 2023.
- [53] C. Zhao, Y. Shen, Z. Chen, M. Ding, and C. Gan, "Textpsg: Panoptic scene graph generation from textual descriptions," in *Proceedings of the IEEE/CVF International Conference on Computer Vision*, 2023, pp. 2839–2850.
- [54] A. Desai, T.-Y. Wu, S. Tripathi, and N. Vasconcelos, "Learning of visual relations: The devil is in the tails," in *Proceedings of the IEEE/CVF International Conference on Computer Vision*, 2021, pp. 15 404–15 413.
- [55] X. Lin, C. Ding, J. Zeng, and D. Tao, "Gps-net: Graph property sensing network for scene graph generation," in *Proceedings of the IEEE/CVF Conference on Computer Vision and Pattern Recognition*, 2020, pp. 3746–3753.
- [56] K. Tang, Y. Niu, J. Huang, J. Shi, and H. Zhang, "Unbiased scene graph generation from biased training," in *Proceedings of the IEEE/CVF conference on computer vision and pattern recognition*, 2020, pp. 3716–3725.
- [57] J. Yu, Y. Chai, Y. Wang, Y. Hu, and Q. Wu, "Cogtree: Cognition tree loss for unbiased scene graph generation," *arXiv preprint arXiv:2009.07526*, 2020.
- [58] S. Abdelkarim, A. Agarwal, P. Achlioptas, J. Chen, J. Huang, B. Li, K. Church, and M. Elhoseiny, "Exploring long tail visual relationship recognition with large vocabulary," in *Proceedings of the IEEE/CVF International Conference on Computer Vision*, 2021, pp. 15 921–15 930.
- [59] M.-J. Chiou, H. Ding, H. Yan, C. Wang, R. Zimmermann, and J. Feng, "Recovering the unbiased scene graphs from the biased ones," in *Proceedings of the 29th ACM International Conference on Multimedia*, 2021, pp. 1581–1590.
- [60] T. Jin, F. Guo, Q. Meng, S. Zhu, X. Xi, W. Wang, Z. Mu, and W. Song, "Fast contextual scene graph generation with unbiased context augmentation," in *Proceedings of the IEEE/CVF Conference on Computer Vision and Pattern Recognition*, 2023, pp. 6302–6311.
- [61] X. Shuai, Y. Shen, S. Jiang, Z. Zhao, Z. Yan, and G. Xing, "Balancefl: Addressing class imbalance in long-tail federated learning," in *2022 21st ACM/IEEE International Conference on Information Processing in Sensor Networks (IPSN)*. IEEE, 2022, pp. 271–284.
- [62] X. Shang, Y. Lu, Y.-m. Cheung, and H. Wang, "Fedic: Federated learning on non-iid and long-tailed data via calibrated distillation," in *2022 IEEE International Conference on Multimedia and Expo (ICME)*. IEEE, 2022, pp. 1–6.
- [63] H. Zhu, J. Xu, S. Liu, and Y. Jin, "Federated learning on non-iid data: A survey," *Neurocomputing*, vol. 465, pp. 371–390, 2021.
- [64] R. Girshick, "Fast r-cnn," in *Proceedings of the IEEE international conference on computer vision*, 2015, pp. 1440–1448.
- [65] R. Krishna, Y. Zhu, O. Groth, J. Johnson, K. Hata, J. Kravitz, S. Chen, Y. Kalantidis, L.-J. Li, D. A. Shamma *et al.*, "Visual genome: Connecting language and vision using crowdsourced dense image annotations," *International journal of computer vision*, vol. 123, pp. 32–73, 2017.
- [66] T.-Y. Lin, M. Maire, S. Belongie, J. Hays, P. Perona, D. Ramanan, P. Dollár, and C. L. Zitnick, "Microsoft coco: Common objects in context," in *Computer Vision—ECCV 2014: 13th European Conference, Zurich, Switzerland, September 6–12, 2014, Proceedings, Part V 13*. Springer, 2014, pp. 740–755.
- [67] D. P. Kingma, "Adam: A method for stochastic optimization," *arXiv preprint arXiv:1412.6980*, 2014.